nature neuroscience

Frontal eye field neurons signal changes in decision criteria

Vincent P Ferrera[1,2], Marianna Yanike[1] & Carlos Cassanello[1]

Flexible links between sensory stimuli and behavioral responses underlie many cognitive processes. One process that contributes to flexible decision-making is categorization. Some categories are innate or overlearned, but, in many cases, category boundaries represent flexible decision criteria that can shift on the fly to adapt to changes in the environment. The ability to shift category boundaries allows decision-making to adapt to changing circumstances. We found that monkeys were able to switch rapidly between two category boundaries when classifying the speed of a moving dot pattern and that neurons in monkey frontal eye field (FEF) changed their activity when the boundary changed. The responses of a subpopulation of FEF neurons that were sensitive to both stimulus and boundary speed were used to classify the stimuli as accurately as the monkeys' performance.

The FEF is a region of prefrontal cortex from which eye movements can be evoked by electrical stimulation with low currents[1,2]. The FEF has been shown to be involved in target selection for voluntary eye movements and spatial attention[3–5]. Recently, FEF neurons have been found to have robust shape selectivity[6], as well as selectivity for direction and speed of motion[7]. They can also exhibit selectivity for features such as color when they are linked to specific motor responses[8,9]. However, it is not clear whether FEF has a role in functions that are thought to be specific to the domain of object vision, such as categorizing a stimulus independently of a specific saccadic eye movement.

Categorical decision-making is an important element of cognitive flexibility. Moveable category boundaries allow for flexible mapping between stimuli and responses. To investigate the role of FEF in categorical decision-making, we developed a speed-categorization task in which monkeys were presented with a random dot motion stimulus and indicated whether the stimulus was moving slow or fast. The task was designed so that the speed categories were independent of the direction of the eye-movement response. The category boundary was determined arbitrarily and the monkeys learned it by trial and error. After the monkeys had learned one boundary speed, the boundary was shifted to a new speed and the monkeys learned the new boundary. Once learned, the monkeys were able to perform the task with two different boundary speeds, one of which was selected randomly on each trial.

We recorded from 96 FEF neurons in two monkeys to determine whether their firing activity was affected by changes in the category boundary. Activity during stimulus presentation was significantly modulated by stimulus speed in roughly one-third of the neurons, and over 40% of FEF neurons had a significant change in activity when the category boundary changed (two-way ANOVA, $P < 0.05$). There was a systematic relationship between stimulus and category preference; cells that responded better to fast stimuli also had higher firing rates on trials with a slower boundary speed. The converse pattern was found for cells that responded better to slower stimuli.

These results provide evidence that FEF activity is influenced by stimulus category and suggest a mechanism for categorical decision-making. Categorical decision-making is thought to involve the accumulation of sensory evidence toward a threshold[10]. Little is known about how this process adapts to different contexts. Our results support the idea that modulation of response gain in neuronal subpopulations with different stimulus selectivities may be a mechanism for implementing context-dependent shifts in decision criteria.

RESULTS

Behavioral evidence of flexible decision-making

To obtain evidence of flexible decision-making in monkeys, we asked whether a shift in the category boundary led to a change in the way monkeys classified the stimuli. Two monkeys performed a speed categorization task (**Fig. 1**) while we recorded neurons in their FEFs. Both subjects were more likely to categorize the stimulus as fast on trials with the slower boundary as compared with the faster boundary (the average number of trials per session was 1,254; **Fig. 2**). The subjects' behavior thus showed a dependence on boundary speed and stimulus speed, suggesting that a shift in the internal reference was used to categorize the stimulus. Note that for each boundary speed, the stimulus probabilities were adjusted so that, on any given trial, the stimulus speed was equally likely to be drawn from the slow category as from the fast category (see Online Methods).

An estimate of the internal reference can be obtained by determining the point of subjective equivalence (PSE), that is, the speed for which the monkey classified the stimulus as being fast on 50% of the trials. This was done by fitting a smooth function to the percentage of fast choices and then finding the speed for which that function yielded a value of 50% (**Fig. 2a**,**b**). The data for each individual session were also fit (**Fig. 2c**). The distributions were well-separated; the average difference between the PSEs was 3.9 deg s^{-1} (paired t test, $P < 10^{-10}$). Despite the apparent overlap of the distributions, there was only one session for which the PSE for slow-boundary trials was greater than the PSE for fast-boundary trials. Nevertheless, it was clear that the means of the distributions did not coincide with the actual category boundaries (**Fig. 2c**). Thus, the data indicate that

[1]Department of Neuroscience and [2]Department of Psychiatry, Columbia University, New York, New York, USA. Correspondence should be addressed to V.P.F. (vpf3@columbia.edu).

Received 28 April; accepted 22 September; published online 25 October 2009; doi:10.1038/nn.2434

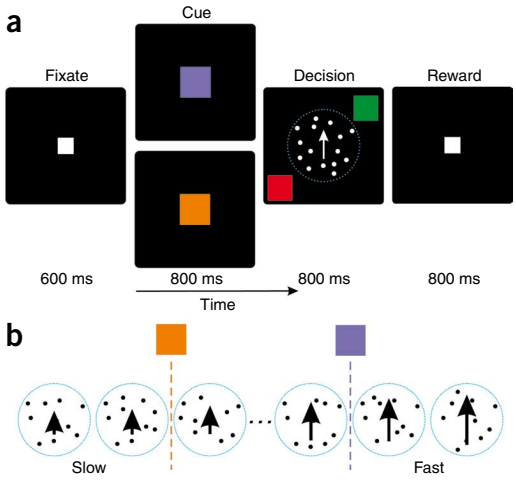

Figure 1 Speed-categorization task. (**a**) Subjects first fixated on a target in the center of the screen and then saw a cue indicating the reference speed (category boundary). A random dot motion stimulus then appeared with two response targets. Subjects made an eye movement to one response target to indicate whether they judged the stimulus speed to be fast (green target) or slow (red target) and received reinforcement on the basis of their response. The stimulus and response targets appeared simultaneously. (**b**) Stimuli and boundaries. The stimulus speed varied from slow (2 deg s^{-1}) to fast (16 deg s^{-1}). The yellow cue indicated a slow reference speed (between 4 and 6 deg s^{-1}), whereas the blue cue indicated a faster reference speed (between 10 and 12 deg s^{-1}).

the monkeys adjusted their internal reference speed when the actual boundary shifted, but fell short of ideal performance.

To determine whether the frequency of boundary shifts affected performance, we compared the overall percent correct for sessions in which the boundary changed once per ~100 trials (blocked, $n = 46$ sessions) with performance during sessions in which the boundary was selected randomly on each trial (random, $n = 50$ sessions). The average percent correct across all trials was 72.7% for blocked versus 73.4% for random sessions (t test, $P = 0.65$). We also classified individual trials as being 'switch' trials if the boundary was different on the previous trial. Performance averaged over all trials was 73.1% correct, whereas performance on switch trials was 72.3% correct. These results indicate that the frequency of changing the category boundary did not affect the monkeys' accuracy and suggest that monkeys were able to shift their internal reference speed on a trial-by-trial basis.

Neuronal activity in FEF during flexible decision-making

To determine whether FEF neurons carry signals related to flexible decision-making, we analyzed the activity of 96 FEF neurons. We examined the time course of neural activity around the decision period for an example neuron (**Fig. 3**). This neuron had a robust response to the stimulus (**Fig. 3a**). This response was strongly modulated by boundary speed. We determined the distribution of spike counts during the first 200 ms of the stimulus presentation, sorted by boundary speed and stimulus speed (**Fig. 3b**). Receiver operating characteristic (ROC) analysis showed that, on the basis of the spike count during the first 200 ms of stimulus presentation, an ideal observer would have been able to correctly guess the boundary speed on 74% of the trials (**Fig. 3c**).

Decision-period neural activity was quantified by computing the average firing rate during the interval between stimulus onset and the behavioral response (**Fig. 4**). In an example session from monkey C, the firing rate was modulated by stimulus speed; the neuron fired more for faster speeds (**Fig. 4b**). The firing rate also depended on the position of the category boundary; across all speeds, the neuron was activated more strongly on trials with the slower boundary. In an example session from monkey F, we observed a complementary pattern of activity from the neuron (**Fig. 4c**,**d**) It responded best to slower speeds, and activity was higher across all stimulus speeds for trials with the faster boundary speed.

The statistical reliability of the effects of stimulus speed and boundary position on firing rate for the example neuron from monkey C (**Fig. 4b**) was tested with a two-way ANOVA and both effects were significant ($P < 0.05$). Rather than signaling stimulus speed *per se*, this neuron might be signaling whether the monkey judged the stimulus as fast or slow relative to the category boundary (reference speed). We analyzed the activity of all 96 FEF neurons by performing a four-way ANOVA on each cell with boundary speed, stimulus speed, outcome (correct or incorrect) and choice (fast or slow) as the explanatory variables (thus, there were two task-related explanatory variables and two behavioral explanatory variables). We found that many FEF neurons were significantly ($P < 0.05$) modulated by one or more variables: 45 neurons (46%) by boundary speed ($P < 0.05$), 36 (37%) by stimulus speed, 25 (26%) by outcome and 12 (13%) by choice (none of the six first-order interactions were significant, $P > 0.05$, for more than 10% of the cells). Hence, more cells were significantly modulated by boundary and stimulus speed than by behavioral variables (outcome and choice).

These results suggest a systematic relationship between the effects of stimulus and boundary speed. For example, the example neuron from monkey C (**Fig. 4b**) had higher firing rates for faster moving stimuli and therefore could be considered a fast-preferring neuron. Other cells (for example, **Fig. 4d**) preferred slower stimuli. We noticed that the fast-preferring cell also tended to respond more on trials with the slow-boundary speed and the slow-preferring cell tended to respond more on trials with the faster boundary. To examine this effect at the population level, we used a linear regression model with boundary

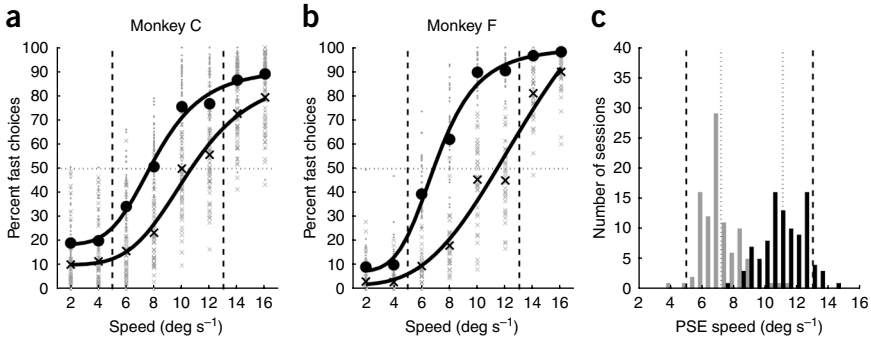

Figure 2 Behavioral performance during the speed-categorization task. (**a**) Percentage of trials for which the stimulus speed was categorized as fast. Dashed vertical lines indicate category boundaries. Small symbols represent data from individual runs, sorted by boundary (circles represent slow boundary, Xs represent fast boundary). Large symbols represent the average performance across all runs. Solid lines represent fits of Naka-Rushton functions. (**b**) Behavioral performance for monkey F. Data are presented as in **a**. (**c**) Distribution of PSEs from Naka-Rushton fits to session-by-session data. Dashed vertical lines are the true boundary speeds; dotted vertical lines are the means of the two PSE distributions.

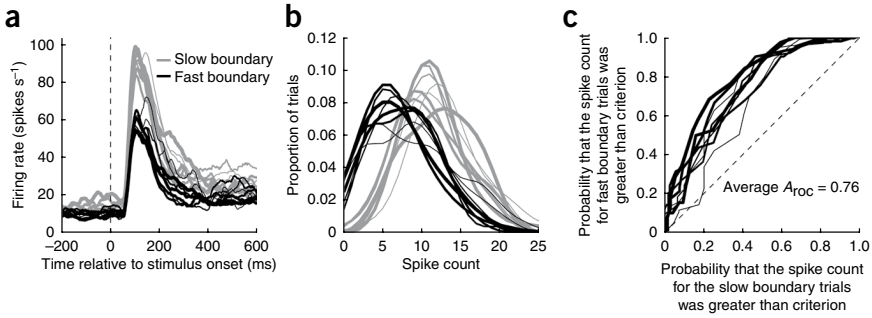

Figure 3 Responses of a category-selective neuron. (**a**) Firing rate as a function of time relative to the onset of the motion stimulus. Trials were sorted by boundary speed and stimulus speed (line thickness increases with stimulus speed). (**b**) Distribution of spike counts during the first 200 ms after stimulus onset. Data are presented as in **a**. (**c**) Discriminability (ROC method) of boundary position on the basis of spike count distributions in **b**. Line thickness increases with stimulus speed, as in **a** and **b**. A_{roc} refers to the area under the curves.

speed and stimulus speed as explanatory variables. The regression model attempted to fit the average firing rate on each trial (FR_i).

$$FR_i = k_0 + k_b S_b + k_s S_s + k_t N_t \quad (1)$$

where S_b is the boundary speed, S_s is the stimulus speed, N_t is the trial number, and k_0, k_b, k_s and k_t are constants. The trial number regressor (N_t) was included to account for slow drifts in neuronal responsiveness that might be confounded with effects of boundary speed. This model provided a significant fit (standard regression of predicted versus actual firing rate, $P < 0.01$) for 87 of 96 (91%) neurons. Note that the model estimates a single value of each constant (k_0, k_b, k_s and k_t) for each neuron.

The four-parameter model of Equation (1) was compared to two six-parameter models that included either trial outcome (correct or incorrect) and category choice (fast or slow) or target position and saccade direction. Adding these covariates improved the fit of the model marginally. However, it did not substantially affect the parameter estimates for boundary and stimulus speed. Details are provided in the **Supplementary Results** and **Supplementary Figures 1–3**.

The data from the example neurons in the monkeys (**Fig. 4b**,**d**) suggest that there might be a systematic relationship between the changes in activity resulting from stimulus speed and those resulting from boundary speed; cells that prefer faster speeds (positive values of k_s) appeared to fire more strongly on trials with the slower boundary speed (negative values of k_b) and vice-versa. This effect should manifest in an inverse relationship between k_b (the coefficient for boundary speed) and k_s (the coefficient for stimulus speed). This trend was confirmed by the parameter estimates obtained by fitting the regression model to each cell. The correlation between k_b and k_s across the population was negative ($r = -0.41$, $P < 0.0001$, $n = 96$; **Fig. 5a**).

The estimates of k_s that we obtained from the regression model were used to classify cells as being fast preferring ($k_s > 0.01$) or slow preferring ($k_s < -0.01$) on the basis of their stimulus preference (this excluded 42 cells for which the speed dependence was very close to zero). A total of 54 of 96 (55%) neurons were classified as either slow preferring ($n = 24$) or fast preferring ($n = 30$). For this subset of neurons, we removed differences in average activity across cells by 'de-meaning', that is, subtracting the mean firing rate during the decision period across all trials from the firing rate on each individual trial. We then averaged the de-meaned firing rates in each class of cell, sorting by stimulus and boundary speed. Even though the cells were classified as being fast or slow based only on stimulus preference, the fast cells had higher firing rates for slow boundary as a group, and the slow cells had higher firing rates for the fast boundary (**Fig. 5b**,**c**). This pattern of activity makes sense; on trials with the slow-boundary speed, the monkey was more likely to categorize most stimulus speeds as fast and cells that prefer faster speeds were therefore more active. Similarly, on trials with the faster boundary speed, the monkey was likely to categorize most of the stimulus speeds as slow; hence, slow preferring neurons were more active.

To demonstrate how this neural modulation (**Fig. 5b**,**c**) can implement shifting decision criteria, we devised a simple algorithm for reading out the responses of the neurons to predict the monkey's behavioral response. The algorithm is based on the idea that fluctuations in a neurons' firing rate represent a vote for one category or the other. If a neuron prefers faster stimuli, then its activity is interpreted as a vote to categorize a stimulus as fast on trials in which its firing rate is significantly greater than its mean firing rate. However, if its firing rate is below average, then it votes to categorize the stimulus as slow. A complementary rule is applied to the activity of neurons that prefer slower moving stimuli. To implement this, we constructed, for each cell, the distribution of firing rates across all trials (including

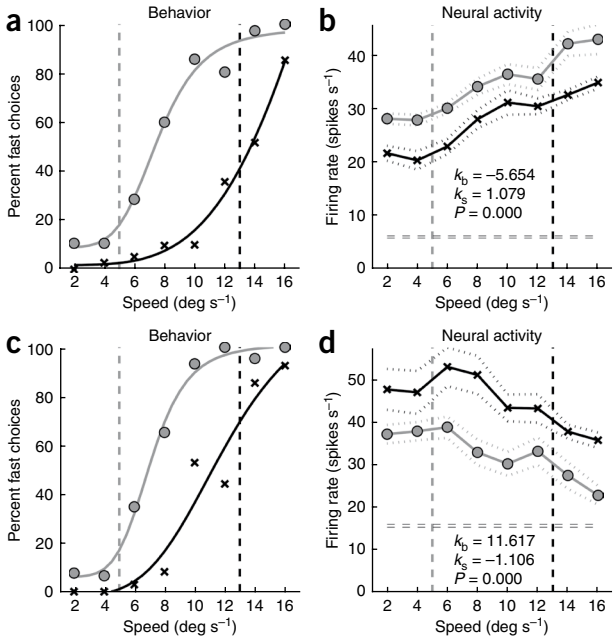

Figure 4 Example data for two recording sessions. (**a**) Behavioral data from one recording session (monkey C). Vertical dashed lines indicate speed boundaries. Gray circles represent trials with the slower boundary and the black Xs are trials with the faster boundary. Smooth curves are Naka-Rushton fits to the behavioral data. (**b**) Response (average firing rate during decision period) of a fast-preferring FEF neuron recorded at the same time as the behavior shown in **a**. Each data point in **b** represents an average across target positions (and hence saccade direction). Symbols indicate the two boundary speeds as shown in **a**. Dashed lines indicate average firing rate ± s.e. Parameter values for the regression model are shown (k_b = coefficient of boundary speed, k_s = coefficient of stimulus speed and P = significance of regression model fit). (**c**) Behavior from one session in a second monkey (F). (**d**) Response of a slow-preferring neuron recorded at the same time.

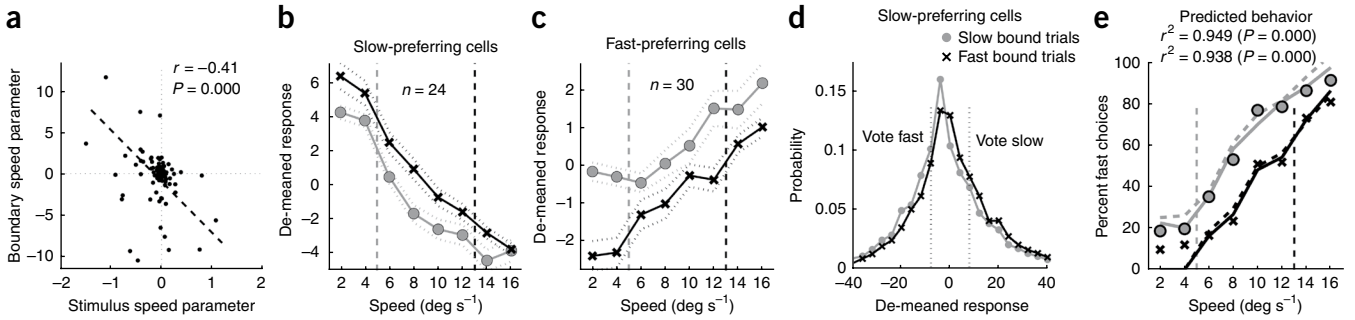

Figure 5 Relationship between neuronal activity and behavior. (**a**) Correlation between regression model parameters. The dashed line represents the best-fitting linear regression. *r* and *P* refer to standard correlation coefficient and significance of regression fit. (**b**,**c**) Population data for fast-preferring (**c**) and slow-preferring (**b**) neurons. *n* is the number of cells in each class. Dashed vertical lines indicate the speed boundaries (slow, gray; fast, black). Symbols indicate the de-meaned responses sorted by boundary speed (slow, gray circles; fast, black Xs). Dashed lines are ± s.e. (**d**) De-meaned firing rate distributions for all slow-preferring neurons sorted by boundary speed. All stimulus speeds are included. Vertical dotted black lines represent the typical threshold used for considering activity as a vote for slow or fast. (**e**) Actual behavioral choices (circles) and choices predicted on the basis of FEF activity (lines). Solid lines are predictions of the threshold model and dashed lines are predictions of the proportional model. r^2 is the correlation between predicted and observed choices.

all stimulus and boundary speeds) and calculated the mean and s.d. of that distribution. Then, on any given trial, we compared the firing rate on that trial (FR_i) to the mean rate $<FR>$, scaling by the s.d. of FR, $\left(\frac{FR_i - <FR>}{\text{s.d.}}\right)$. If that number was greater than a threshold, δ(which was the same for all neurons), then it represented a vote for the cell's preferred speed (fast or slow). If the number was smaller than $-\delta$, then it represented a vote for the opposite category.

To illustrate this, we determined the distributions of de-meaned firing rates for a population of slow-preferring neurons (**Fig. 5c**) along with the thresholds for voting fast or slow. Not every neuron voted on every trial. If a neuron's firing rate on a given trial was within $\pm\delta$ of its mean, it did not cast a vote on that trial. In addition to this threshold model, we also simulated a proportional model in which the probability of each response category was linearly proportional to the normalized activity of the cell.

We applied both algorithms to the subset of neurons described above (**Fig. 5a**,**b**). For the threshold model, the correlation between the predicted and actual choice probabilities was strong and significant ($r^2 = 0.95$, $P < 0.0001$, $n = 16$; **Fig. 5d**). Similar results were obtained for the proportional model ($r^2 = 0.94$, $P < 0.0001$, $n = 16$; **Fig. 5d**). Thus, a subpopulation consisting of 55% FEF neurons and selected only on the basis of their stimulus selectivity was sufficiently strongly modulated by category boundary position to quantitatively account for subjects' behavioral choices.

It is important to note that the category selectivity of the neuron was independent of the eye movements that the monkey made to indicate his choices. The monkey signaled his choice by making a saccadic eye movement to one of two response targets. The targets were different colors (green or red) and the monkey learned that green indicated fast and red indicated slow. However, neither target was in the receptive/movement field of the neuron. Furthermore, the positions of the targets were randomized so that a given target color was not always associated with the same movement. A similar strategy was used previously[11] to distinguish perceptual decisions from motor responses in the superior colliculus.

DISCUSSION

A central issue in the neurobiology of decision-making is how sensory representations are transformed into categorical or 'decision-based' representations. A categorical decision process is one that maps a continuous sensory input onto a finite number of responses in a many-to-one manner (that is, multiple stimuli are associated with a single behavioral response; different classes of stimuli map onto different behavioral responses). Categorical decisions are closely linked with object recognition, abstract concept formation[12] and the development of language[13,14]. Through a combination of psychophysical[15] and neurophysiological approaches[16,17], we are now beginning to understand the neural basis of categorical decision-making.

Visual categorization is often associated with the ventral visual-processing stream, which includes visual areas of the inferior temporal lobe and is involved in object recognition[18]. This view is supported by several physiological studies[19–21], as well as the observation of category-specific agnosias following temporal lobe lesions[22]. However, there is increasing evidence that the dorsal visual pathway might be involved in object recognition[23] and visual categorization[17].

The dorsal and ventral visual pathways both send anatomical projections to the FEF[24]. FEF neurons have recently been found to have robust shape selectivity[6], as well as selectivity for direction and speed of motion[7]. They can also exhibit selectivity for features such as color when they are linked to specific motor responses[8,9]. Our results suggest that FEF may be involved in functions that are thought to be specific to the domain of object vision, such as categorizing a stimulus independently of a specific saccadic eye movement.

Categorization is closely linked to feature-selective attention. Recent work suggests that attention is drawn to informative features during categorization tasks[25]. It is possible that our results reflect an enhanced representation of stimulus features that are relevant to the categorical decision. Moreover, it may be possible to not only attend to a particular feature (that is, speed), but to limit attention to a subset of values in that stimulus dimension, that is, to attend only to faster or slower speeds, and thereby enhance the activity of cells whose selectivity is most relevant to the decision at hand.

METHODS

Methods and any associated references are available in the online version of the paper at http://www.nature.com/natureneuroscience/.

Note: Supplementary information is available on the Nature Neuroscience website.

ACKNOWLEDGMENTS

We would like to thank J. Schall, R. Ratcliff, F. Pestilli, J. Grinband, T. Teichert, C. Barberini and M. Phillips for comments on a preliminary version of this manuscript. This research was supported by US National Institutes of Health grant MH59244 (V.P.F.), the Gatsby Institute (V.P.F.), the National Alliance for Research on Schizophrenia and Depression (V.P.F.) and the Robert Leet and Clara Guthrie Patterson Trust (M.Y.).

AUTHOR CONTRIBUTIONS

V.P.F., M.Y. and C.C. designed the experiments, analyzed the data and wrote the manuscript. M.Y. and C.C. carried out the experiments.

Published online at http://www.nature.com/natureneuroscience/.
Reprints and permissions information is available online at http://www.nature.com/reprintsandpermissions/.

1. Ferrier, D. *The Functions of The Brain* (Putnam. New York, 1876).
2. Bruce, C.J., Goldberg, M.E., Bushnell, M.C. & Stanton, G.B. Primate frontal eye fields. II. Physiological and anatomical correlates of electrically evoked eye movements. *J. Neurophysiol.* **54**, 714–734 (1985).
3. Schall, J.D., Hanes, D.P., Thompson, K.G. & King, D.J. Saccade target selection in frontal eye field of macaque. I. Visual and premovement activation. *J. Neurosci.* **15**, 6905–6918 (1995a).
4. Moore, T. & Armstrong, K.M. Selective gating of visual signals by microstimulation of frontal cortex. *Nature* **421**, 370–373 (2003).
5. Thompson, K.G., Biscoe, K.L. & Sato, T.R. Neuronal basis of covert spatial attention in the frontal eye field. *J. Neurosci.* **25**, 9479–9487 (2005).
6. Peng, X., Sereno, M.E., Silva, A.K., Lehky, S.R. & Sereno, A.B. Shape selectivity in primate frontal eye field. *J. Neurophysiol.* **100**, 796–814 (2008).
7. Xiao, Q., Barborica, A. & Ferrera, V.P. Radial motion bias in macaque frontal eye field. *Vis. Neurosci.* **23**, 49–60 (2006).
8. Bichot, N.P., Schall, J.D. & Thompson, K.G. Visual feature selectivity in frontal eye fields induced by experience in mature macaques. *Nature* **381**, 697–699 (1996).
9. Ferrera, V.P., Cohen, J.K. & Lee, B.B. Activity of prefrontal neurons during location and color delayed matching tasks. *Neuroreport* **10**, 1315–1322 (1999).
10. Ratcliff, R. & McKoon, G. The diffusion decision model: theory and data for two-choice decision tasks. *Neural Comput.* **20**, 873–922 (2008).
11. Horwitz, G.D., Batista, A.P. & Newsome, W.T. Representation of an abstract perceptual decision in macaque superior colliculus. *J. Neurophysiol.* **91**, 2281–2296 (2004).
12. Miller, E.K., Nieder, A., Freedman, D.J. & Wallis, J.D. Neural correlates of categories and concepts. *Curr. Opin. Neurobiol.* **13**, 198–203 (2003).
13. Gopnik, A. & Meltzoff, A. The development of categorization in the second year and its relation to other cognitive and linguistic developments. *Child Dev.* **58**, 1523–1531 (1987).
14. Campbell, R.N. Categorization, early concepts and first language acquisition. in *Encyclopedia of Language & Linguistics 4* (eds Asher, R. & Simpson, J.M.Y.) 1899–1904 (Elsevier, Amsterdam, 1994).
15. Ashby, F.G. & Maddox, W.T. Human category learning. *Annu. Rev. Psychol.* **56**, 149–178 (2005).
16. Freedman, D.J., Riesenhuber, M., Poggio, T. & Miller, E.K. Categorical representation of visual stimuli in the primate prefrontal cortex. *Science* **291**, 312–316 (2001).
17. Freedman, D.J. & Assad, J.A. Experience-dependent representation of visual categories in parietal cortex. *Nature* **443**, 85–88 (2006).
18. Maunsell, J.H. & Newsome, W.T. Visual processing in monkey extrastriate cortex. *Annu. Rev. Neurosci.* **10**, 363–401 (1987).
19. Kreiman, G., Koch, C. & Fried, I. Category-specific visual responses of single neurons in the human medial temporal lobe. *Nat. Neurosci.* **3**, 946–953 (2000).
20. Sigala, N. & Logothetis, N.K. Visual categorization shapes feature selectivity in the primate temporal cortex. *Nature* **415**, 318–320 (2002).
21. Freedman, D.J., Riesenhuber, M., Poggio, T. & Miller, E.K. A comparison of primate prefrontal and inferior temporal cortex during visual categorization. *J. Neurosci.* **23**, 5235–5246 (2003).
22. Farah, M.J. *Visual Agnosia* (MIT Press, Cambridge, Massachusetts, 2004).
23. Sereno, A.B. & Maunsell, J.H. Shape selectivity in primate lateral intraparietal cortex. *Nature* **395**, 500–503 (1998).
24. Schall, J.D., Morel, A., King, D.J. & Bullier, J. Topography of visual cortex connections with frontal eye field in macaque: convergence and segregation of processing streams. *J. Neurosci.* **15**, 4464–4487 (1995).
25. Blair, M.R., Watson, M.R., Walshe, R.C. & Maj, F. Extremely selective attention: eye-tracking studies of the dynamic allocation of attention to stimulus features in categorization. *J. Exp. Psychol. Learn. Mem. Cogn.* **35**, 1196–1206 (2009).

ONLINE METHODS

Animals. Experiments were performed on two adult male rhesus monkeys (*Macaca mulatta*) weighing between 6 and 8 kg. All methods were approved by the Institutional Animal Care and Use Committee at Columbia University and the New York State Psychiatric Institute. Monkeys were prepared for experiments by surgical implantation of a post used for head restraint and a recording chamber to give access to the cortex. Eye position was recorded using a monocular scleral search coil. All surgical procedures were performed using aseptic technique and general (1–3% isoflurane, vol/vol) anesthesia. Monkeys were trained to sit in a primate chair for the duration of the experiment with their heads restrained and perform the behavioral tasks. Correct performance of the task was reinforced by liquid reward.

Visual stimulation and eye movement recording. Visual stimuli were generated and controlled by a Cambridge Research Systems VSG2/3F video frame buffer. The output from the video board was displayed on a calibrated 37-inch color monitor (Mitsubishi) with a 60-Hz non-interlaced refresh rate. The monitor stood at a viewing distance of 24 inches so that the display area subtended roughly 40 degrees horizontally by 30 degrees vertically. The spatial resolution of the display was 1,280 pixels by 1,024 lines. The visual stimuli used during the task consisted of a 0.5-deg square white fixation target, a 1.0-deg circular yellow cue or square blue cue, an 8-deg diameter round patch of random moving dots, and a 1.0-deg square red or green saccade target. All stimuli were presented on a uniform black background. The frame buffer was programmed to send out digital pulses (frame sync) for timing purposes at the beginning of each video frame in which a target was turned on or off. These pulses were recorded by the computer using a hardware timer and stored together with the neuronal and eye movement data.

Eye position was monitored using a monocular scleral search coil system (CNC Engineering). The eye position signals were then digitally sampled by computer at 1 kHz per channel, digitized with 12-bit resolution and stored on a disk for offline analysis. Velocity was computed from eye-position information using a differentiating filter algorithm. Eye position and velocity were used to estimate saccade parameters. Saccade onsets and offsets were computed using an acceleration criterion.

Neuronal recording and electrical stimulation. Recording chambers (20 mm in diameter) were implanted on the skull overlying the arcuate sulcus, positioned at stereotaxic coordinates 25 anterior, 15 lateral. At the start of each recording session, a hydraulic microdrive (Kopf) was mounted on the recording chamber. Recordings were made using platinum-iridium electrodes with impedances of 0.1–1 Mohm. Signals from the microelectrode were amplified, filtered and monitored on an oscilloscope and audio monitor. A time-amplitude window discriminator converted extracellular action potentials into digital pulses (TTL), which were sampled by the computer with 0.01-ms time resolution. Units were isolated on the basis of waveform. When a unit was isolated, stimulus parameters such as the position and size of the moving dot pattern were adjusted to optimize its response. Neuronal spike trains were collected and stored along with eye-position data.

Electrical microstimulation was used to map the region of cortex from which neuronal recordings were obtained in each monkey. Sites in peri-arcuate cortex were stimulated through the same electrode used to record neuronal activity. The stimulation consisted of a train of 0.2-ms biphasic pulses at a rate of 350 pulses per s delivered by an optically isolated pulse stimulator (AM Systems). The output of the stimulator was gated by a computer-generated TTL level so as to be synchronized with other trial events. The current threshold for evoking saccades was determined by stimulating during a fixation task[26]. The threshold was defined as the current level at which involuntary saccades were evoked on about half the stimulation trials[2]. The mean threshold was 43 μA.

For all sites, electrically evoked saccades were almost always contraversive and showed a mediolateral gradation of amplitudes[2]. In addition, the evoked saccade direction rotated systematically as the depth of the electrode changed. These features of the saccade amplitude and direction map are characteristic of the FEF. A structural magnetic resonance imaging for one monkey is provided in the **Supplementary Methods** and **Supplementary Figure 4**.

Behavioral procedures. After collecting data for the memory-guided saccade task (**Supplementary Methods** and **Supplementary Fig. 4**), we switched to the speed categorization task (**Fig. 1**). In this task, the monkeys viewed a random dot motion stimulus and categorized its speed as being slow or fast. The response was indicated by making a saccadic eye movement to either a red or green response target. The monkeys learned to associate the response category with the target color (slow, red; fast, green). A correct response was reinforced with a few drops of water or fruit juice and a high auditory tone. An incorrect response was signaled with a low tone.

The stimulus speed was selected at random on every trial from a set of eight speeds (2, 4, 6, 8, 10, 12, 14 and 16 deg s^{-1}). Subjects classified the speed of motion as slow or fast according to boundaries (reference speeds) that were learned by trial and error. The subjects learned two boundaries (**Fig. 1b**). One boundary was between 4 and 6 deg s^{-1} (slow reference) and the other was between 12 and 14 deg s^{-1} (fast reference). On any given trial, only one boundary was used, and the boundary was either fixed for a block of trials or selected at random on every trial. In 46 recording sessions, the category boundary was changed roughly once every 100 trials (blocked condition). In 50 sessions, the category boundary was selected randomly on each trial (random condition). The boundary was indicated by a cue presented at the beginning of the trial. A yellow circle indicated that the slow reference was in effect and a blue square indicated the fast reference.

Subjects indicated their categorical decision (slow or fast) by making a saccadic eye movement to one of two response targets. The targets were red and green and the subject learned the rule that slow indicated red and fast indicated green. The positions of the response targets were randomized so that there was no systematic relationship between the slow and fast categories and the direction of the eye movement.

It should also be noted that the boundary positions split the stimulus set into unequal parts; for each boundary, there were two stimulus speeds in one category and six in the other. This potentially affects the prior probability of each stimulus category. For example, given the slow reference, the monkey might be able to respond fast on every trial, regardless of the stimulus, and be correct 75% of the time. To bring the guessing rate back down to 50%, we altered the stimulus probability. For the slow reference, speeds of 2 and 4 deg s^{-1} were presented three times as frequently as 6, 8, 10, 12, 14 and 16 deg s^{-1}. For the fast reference, 14 and 16 deg s^{-1} were presented three times as frequently as the other speeds. Thus, for each reference speed, both response categories were equally likely to be correct. Over all trial conditions, the extreme speeds (2, 4, 14 and 16 deg s^{-1}) were presented twice as often as the intermediate speeds (6, 8, 10 and 12 deg s^{-1}).

The monkey had 800 ms to acquire the initial fixation target. The cue was then presented for 800 ms. Immediately after the cue, the motion stimulus and response targets were presented for 800 ms; this was the decision period. The subject could respond at any time during this interval, but the reward was not given until after the decision period had elapsed. Thus, the subject could not speed the reward by responding more quickly.

The geometry of the display was such that the response targets were always presented to either side of the random dot stimulus. The direction of dot motion was aligned with the axis orthogonal to the axis defined by the response targets. Both directions of motion along this axis were used and the direction was chosen randomly on each trial.

Data analysis. The speed-categorization task had 64 conditions comprising different combinations of stimulus direction and speed, boundary speed, and response target position. Except for the reference speed, all stimulus conditions were presented interleaved randomly in a block of trials.

For analysis of neural activity, each trial of the speed categorization task was divided into four time epochs: fixation interval (100 ms before cue onset), cue interval (800 ms after the onset of the cue and before the stimulus presentation), decision interval (the time after stimulus and response target onset and before the onset of the choice saccade) and post-saccadic interval (100 ms after the end of the saccade). The average firing rate was computed in each time window. The number of repetitions of each trial condition was typically ten or more. For the purposes of this study, only neuronal activity during the decision interval was considered.

26. Opris, I., Barborica, A. & Ferrera, V.P. On the gap effect for saccades evoked by electrical microstimulation of frontal eye fields in monkeys. *Exp. Brain Res.* **138**, 1–7 (2001).

doi:10.1038/nn.2434

Frontal Eye Field Neurons Signal Changes in Decision Criteria

Vincent P. Ferrera, Marianna Yanike, Carlos Cassanello

SUPPLEMENTARY RESULTS

Spatial bias

Most FEF neurons have strong spatial selectivity both for visual target location and/or for saccade direction and amplitude. In the speed categorization task, there were two locations for saccade targets. We generally attempted to place both saccade targets outside the receptive/movement field of the neuron being recorded. However, it was still possible that a neuron could fire somewhat more strongly prior to saccades directed toward one target location than the other, particularly if the targets were near the edges of the RF/MF. **Fig. S1** illustrates a case where one target location might evoke a stronger response than the other. In fact, across the population of neurons recorded, saccades

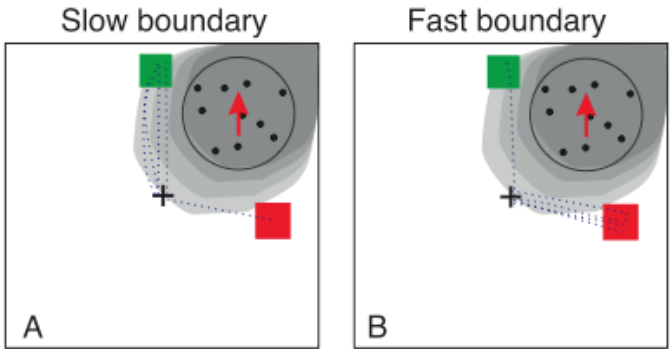

Figure S1. Worst-case scenario for spatial bias confound. **A)** One response target (green) has greater overlap with the RF/MF (gray shaded region) than the other target (red), and the monkey's saccades (dotted blue lines) are biased toward the "preferred" target location. **B)** Same target configuration, but monkey's saccades are biased toward the "non-preferred" location.

Nature Neuroscience: doi:10.1038/nn.2434

directed toward one target location did tend to evoke a response that averaged 19% stronger than the response at the weaker location. This effect was small, but significant across the population (paired t-test, $p < 10^{-6}$).

Even though the experiment was designed to dissociate categorical from spatial responses (by randomizing the response targets between the two locations), it is possible that subjects could have systematic biases. It is possible that this spatial response bias, if combined with a behavioral bias, could be confounded with categorization effects. This would happen, for example, if the monkey systematically selected the target at the stronger location when one boundary was in effect, and chose the target at the weaker location when the other boundary was in effect. **Fig. S1** illustrates the possibility that the monkey could make more saccades to the "preferred" target location on "slow" boundary trials (**Fig. S1A**), but have the opposite bias on "fast" boundary trials (**Fig. S1B**).

To test this, we calculated the proportion of trials for which the monkey chose the target at the stronger location. This was accomplished by first finding the target location that produced the strongest neuronal response for each cell, and then calculating the percentage of responses directed to that location as opposed to the opposite location. **Fig. S2** shows the spatial response bias of each subject, sorted by stimulus and boundary speed, relative to the preferred spatial location of each neuron. To account for the categorization effects, there would have to be a systematic difference between the distribution of the red and blue data points. **Fig. S2 A,B** shows data for the subset of cells that responded more strongly when the slow boundary was in effect (n = 51). If this were due to a spatial bias, then the red data points would show a tendency to lie

Nature Neuroscience: doi:10.1038/nn.2434

above the blue points. This is not evident either at the level of individual sessions (small circles) or in the aggregate data (solid lines). **Fig. S2 C,D** shows data for the subset of cells that responded more strongly when the fast boundary was in effect (n = 45). In this case, the blue points should lie above the red. These data show that the monkeys had no systematic spatial biases that could account for the effects of boundary speed.

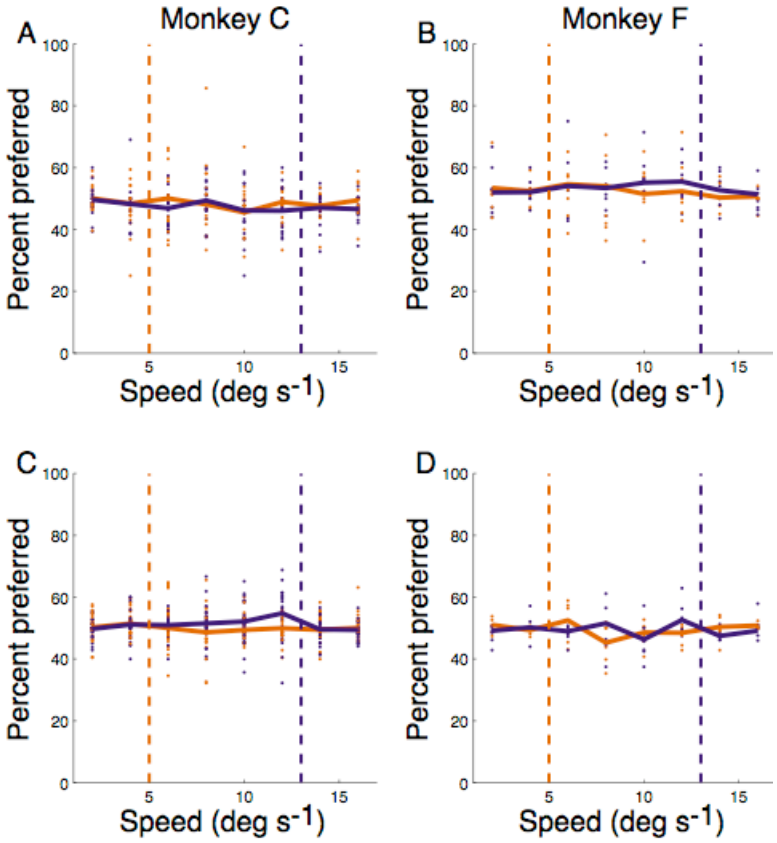

Figure S2. Control for spatial bias. **A)** Percentage of saccades directed toward the target at the "preferred" location of the cell. Red and blue dots are within session averages sorted by stimulus and boundary speed. Solid lines are across-session averages. Dashed vertical lines indicate the two boundary speeds. The data in this panel represent fast-preferring neurons in monkey C. **B)** Same format as A, showing fast-preferring cells in monkey F. **C)** Slow-preferring cells in monkey C. **D)** Slow-preferring cells from monkey F.

As another test for the robustness of boundary and stimulus speed effects, we performed a 4-way ANOVA with boundary speed, stimulus speed, target position and saccade direction as the explanatory variables. Target position refers to the position of the correct target and hence differs from saccade direction on incorrect trials. At the p <

Nature Neuroscience: doi:10.1038/nn.2434

0.05 level, the following numbers of cells showed significant effects: 45 for boundary speed, 37 for stimulus speed, 32 for target position, 43 for saccade direction. None of the interactions were significant for more than 12 cells. A 2-way ANOVA was also performed with only boundary and stimulus speed as the independent variables. In the 2-way analysis, 45 cells were significant for boundary speed ($p < 0.05$) and 36 for stimulus speed (none of the 6 first-order interactions was significant, $p<0.05$, for more than 10% of the cells, except for the interaction between target position and saccade direction, which was significant for 22% of cells). All of the cells that were significant for boundary speed in the 2-way ANOVA also showed a significant boundary effect in the 4-way ANOVA when target position and saccade direction were included as covariates. Thus, while target position and saccade

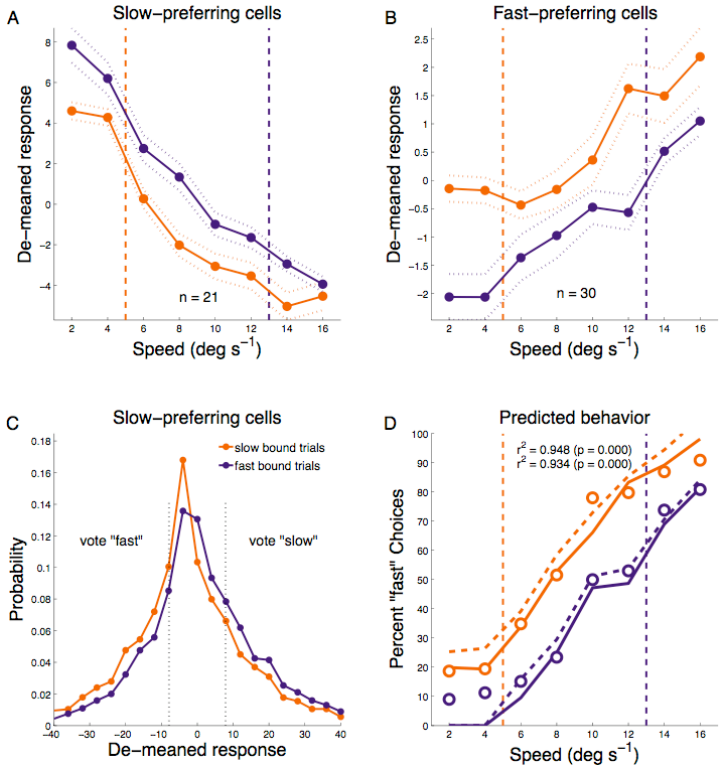

Figure S3. Population data for **A)** "fast" and **B)** "slow" preferring neurons. "n" is the number of cells in each class is given. **C)** De-meaned firing rate distributions for all slow-preferring neurons sorted by boundary speed. All stimulus speeds are included. Vertical dotted black lines represent the typical threshold used for considering activity as a vote for "slow" or "fast." **D)** Actual behavioral choices (circles) and choices predicted based on FEF activity (lines). Solid lines are predictions of the "threshold" model, dashed lines are predictions of the "proportional" model.

Nature Neuroscience: doi:10.1038/nn.2434

direction were significant for 33% and 45% of the cells, respectively, these effects did not reduce the significance of boundary and stimulus speed.

We also performed a regression analysis by adding target and saccade direction co-variates to the model of Eqn 1. The 6-parameter model provided a significant fit ($p < 0.01$) for all but 6 neurons. The 6-parameter model provided a better fit than the 4-parameter model for 87 neurons, and a worse fit for 9 neurons. On average, the 6-parameter model improved the correlation between predicted and actual firing rate by 23% over the 4-parameter model. This improvement was significant (paired t-test $p < 0.00001$).

The effects of target position and saccade direction were expected and consistent with the small (avg 19%) but significant bias in neuronal responses. However, these effects did not degrade the encoding of boundary and stimulus speed. **Fig. S3** is analogous to **Fig. 5** from the main body of the paper. The only difference is that the neurons were sorted based on the 6-parameter, rather than 4-parameter model. The results for both models are nearly identical.

Effects of behavioral choice and outcome

To determine if neurons encode both the boundary speed and the stimulus speed even when one controls for the subject's final choice, we ran all combinations of 1-, 2-, 3-, and 4-way ANOVAS with the following explanatory variables: boundary speed, stimulus speed, choice (fast/slow), and outcome (correct/incorrect). The results were highly consistent. In all analyses, 45 cells had a significant effect of boundary speed ($p<0.05$) and 36 were significant for stimulus speed. These numbers were the

Nature Neuroscience: doi:10.1038/nn.2434

same with and without outcome and choice as covariates. The results for the 4-way ANOVA at $p<0.05$ were as follows: boundary speed: 45 cells; stimulus speed: 36 cells; outcome: 25 cells; choice: 12 cells. These results suggest that more cells were modulated by boundary and stimulus speed than by outcome and choice.

The ANOVA results were consistent with regression analyses. In particular, we compared the 4-parameter model of Eqn 1 with 5- and 6-parameter models that included behavioral outcome and choice as additional regressors. The results were consistent across all models, so we will only discuss the 6-parameter model (explanatory variables = boundary speed, stimulus speed, outcome, choice, trial number). Compared to the 4-parameter model (Eqn 1), adding the additional behavioral variables improved the fit of the model for 64 cells and worsened the fit for 32 cells. The mean difference (6-parameter fit – 4-parameter fit) was +7%. Fit was measured by computing the correlation between predicted and actual firing rate. The improvement was rather small considering the 50% increase in the number of parameters.

As far as the results shown in **Fig. 5**, adding the behavioral variables to the regression model changed things only slightly. The most notable change was that the negative correlation between the boundary speed and stimulus speed parameters became a bit stronger (-0.41 for the 4-parameter model to -0.44 for the 6-parameter model). This is important because it is this negative relationship that allows one to predict the animal's behavior based on neural activity. The numbers of slow (n = 24) and fast (n = 32) cells did not change appreciably, nor did the fit between predicted and actual behavior ($r^2 = 0.952$).

Nature Neuroscience: doi:10.1038/nn.2434

Time-dependence of stimulus and category effects

Response times for the speed categorization task were typically about 400 ms (measured as the time from stimulus onset to saccade onset). To gain a sense of the relative timing of boundary and stimulus speed signals, we subdivided this interval into two 200-msec subintervals, one starting at stimulus onset (VIS) and the other ending at saccade onset (SACC). The ANOVA and regression model analyses were performed on activity (average firing rate) in these two intervals. A 4-way ANOVA found significant ($p < 0.05$) effects during the VIS interval for the following numbers of cells: 39 boundary speed; 25 stimulus speed; 9 target direction; 23 saccade direction.

The number of cells showing a significant boundary speed effect was similar to that obtained with a 2-way ANOVA using either the entire decision period (n = 45) or just the VIS interval (n = 39). The number of cell showing a significant boundary speed effect during the SACC interval was 43 and 42 for the 4- and 2-way ANOVAs, respectively. Hence, the boundary speed effect is stable over time.

The number cells with a significant stimulus speed effect in the VIS interval was the same (n = 25) for 2- and 4-way ANOVAs. This number increased 40% (to n = 42) for activity in the SACC interval. This number was also independent of whether target direction and saccade direction were included as covariates. Hence, the effect of stimulus speed was stronger during the SACC interval than the VIS interval.

The regression analysis confirmed these results. Estimates of the boundary speed parameter (k_b) were similar for the VIS and SACC interval. They averaged 1.89 spikes s^{-1} for the VIS interval and 1.96 spikes s^{-1} for the SACC interval (mean absolute value). This result was obtained with the 4-parameter model (Eqn 1), but also held for

Nature Neuroscience: doi:10.1038/nn.2434

the 6-parameter models that included outcome and choice or target and saccade direction as additional covariates.

In contrast, the parameter estimate for stimulus speed was much larger during the SACC interval (0.34 spikes/sec per deg s^{-1}) than the VIS interval (0.19 spikes s^{-1} per deg s^{-1}). This result was consistent across all 4- and 6- parameter regression models. Hence, the effect of stimulus speed increased with time during the decision interval.

As the influence of stimulus speed increased, so did the negative correlation between the parameter estimates for stimulus and boundary speed (k_s and k_b in Eqn 1). In the VIS interval, this correlation was –0.26 ($p = 0.012$), and increased to –0.56 ($p < 0.0001$) in the SACC interval.

These results are consistent with the idea that the boundary speed effect is established prior to the appearance of the stimulus. This makes sense because the boundary cue appears 800 msec before the motion stimulus. In some cells, the stimulus speed effect is present early, but in others it takes more time to evolve. In either case, stimulus speed signals can be modulated by a boundary speed signal that is present throughout the decision period. These results further support the idea that differential modulation of sensory signals may be a mechanism for implementing decision criteria.

Nature Neuroscience: doi:10.1038/nn.2434

SUPPLEMENTARY METHODS

Anatomical location of recording sites

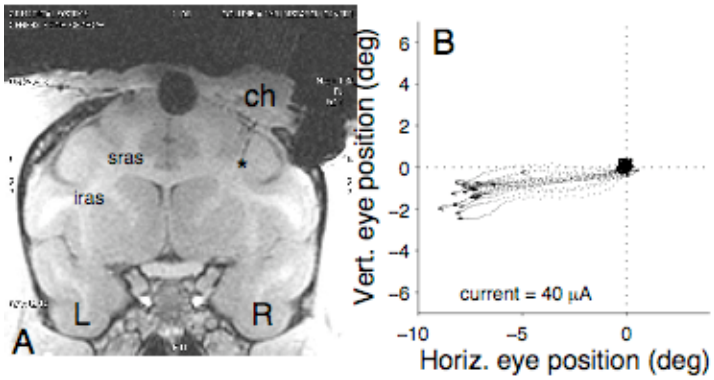

Figure S4. Anatomic localization of recording sites. **A)** Structural MRI of monkey F showing coronal slice at the level of the arcuate sulcus (iras – inferior ramus of arcuate, sras – superior ramus). A recording chamber (ch) and electrode track are shown in the right hemisphere. **B)** Saccades evoked by stimulation of the site labeled with the asterisk in A. The current level was 40 uA.

Structural MRI was used to reconstruct electrode penetrations. Monkeys were sedated with ketamine (10 mg/kg), anesthetized with isoflurane (13%), and placed in an MR-compatible stereotaxic frame inside the scanner. An SPGR pulse sequence was used on a GE 1.5T TwinSpeed scanner. **Figure S4A** shows a coronal structural MRI from one monkey (F). The anterior-posterior level of the slice is 26.0 mm anterior to the ear canals. The superior (s) and inferior rami (i) of the arcuate sulcus are indicated. There are two clearly visible electrode tracks in the anterior bank of the arcuate sulcus on the right side. At the site marked with the asterisk, contraversive saccades were evoked at a current of 40 microamps (**Fig. S4B**).

Neuron Classification

The activity of FEF neurons can be classified as visual-, visual-movement-, or movement-related based on whether it is more strongly associated with a visual

Nature Neuroscience: doi:10.1038/nn.2434

stimulus or with a saccadic eye movement (Bruce and Goldberg, 1985). To classify cells in this manner, we trained monkeys to perform a delayed, memory-saccade task (MEM). This task was also used to 1) determine if the neuron responded to visual targets and/or prior to saccadic eye movements, and 2) determine the location in the visual field that yielded the strongest response.

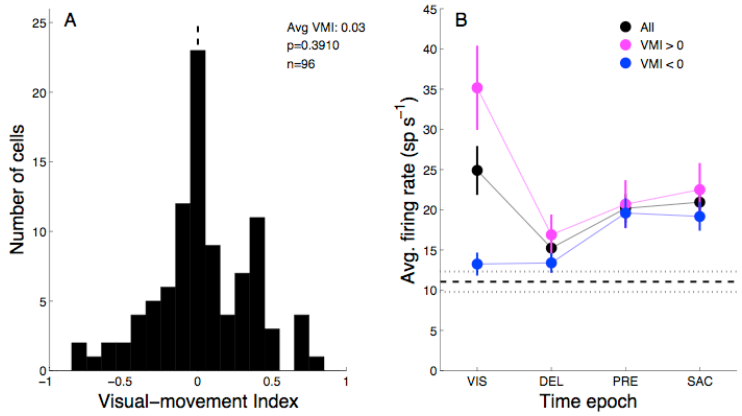

Figure S5. Classification of FEF neurons based on activity during memory-saccade task. **A)** Distribution of visual-motor indices (VMI). Most cells were recording with 2 target eccentricities and a VMI was computed for each eccentricity, hence the y-axis label refers to the number of recordings rather than the number of cells. **B)** Avg. firing rate for visual (VIS), delay (DEL), pre-saccade (PRE) and peri-saccade (SAC) time intervals. Black symbols include all cells, blue includes only cells with VMI < 0, magenta includes cells with VMI > 0.

In the MEM task, monkeys made saccades to the remembered location of a visual cue. The cue location varied among eight positions, equally spaced (45 deg). Typically, 2 different target eccentricities were used. At the beginning of each trial the monkey fixated a small red square. A peripheral cue was flashed for 250 ms followed by a variable delay (750-1250ms) during which the fixation target remained on and the monkey maintained fixation within a 2 x 2 deg window. At the end of the delay, the fixation target disappeared and the monkey was allowed up to 600 ms to make a saccade to the remembered location of the cue. After the 600 ms saccade interval, and if the monkey's

Nature Neuroscience: doi:10.1038/nn.2434

memory-saccade was within a 3 x 3 deg window centered on the cue location, the cue re-appeared to provide feedback to the monkey and corrective saccades were generally made at this time. More details on this task have been given elsewhere (Cassanello and Ferrera 2007b).

For analysis, each MEM trial was divided in five time intervals including background, visual, delay, pre and peri-saccadic intervals. The intervals were defined as follows: background – 100 msec before the onset of the visual cue; visual – 50-200 msec after onset of visual cue; delay – time between offset of visual cue and "go" signal for saccade; pre-saccade – 150 msec before saccade; peri-saccadic 50 msec before the saccade to 100 msec after.. Average firing rate within each interval is indicated by the variables B, V, D, P and S. We computed a visuomotor index to classify neurons as follows:

(Eqn S1) $$VMI = (V - M) / (V + M)$$

This index ranges from –1.0 (pure movement cell) to 1.0 (pure visual cell). In each case, the firing rates were calculated using the trial condition that produced the maximum overall response, i.e. the preferred target location or saccade metric (direction and amplitude). If a cell was recorded with multiple target eccentricities, the VMI was calculated separately for each eccentricity.

The distribution of VMI's across the population of neurons was not significantly biased toward visual or movement (**Fig. S5A**). The average firing rates for the visual, delay, pre-saccade and peri-saccade intervals are shown in **Fig. S5B**. The average firing rates around the time of the saccade were similar for cells with VMI > 0 and those with VMI < 0. The cell classes were better distinguished by activity during the visual

Nature Neuroscience: doi:10.1038/nn.2434

interval. Bruce and Goldberg (1985) reported that 60% of FEF neurons were classified as pure movement or visual-movement neurons, and 40% were purely visual. However, it is possible that pure movement and pure visual neurons are somewhat under-represented in our sample.

To determine if there was a relationship between cell class and stimulus or boundary speed selectivity, we sorted the neurons into 3 groups: those with VMI < -0.3 ("movement" cells), -0.3 < VMI < 0.3 ("visual-movement"), and VMI > 0.3. We calculated the magnitude of the boundary and stimulus speed parameter estimates for each neuron and compared between groups using a Wilcoxon rank-sum test. None of the between group comparisons were significant ($p < 0.05$). We also computed the correlation between VMI and the magnitude of the boundary and stimulus speed parameter estimates. Neither correlation was significant ($p < 0.05$).

Nature Neuroscience: doi:10.1038/nn.2434